Size matters: Physiological sensitivity of the scallop *Argopecten purpuratus* to seasonal cooling and deoxygenation upwelling-driven events

Laura Ramajo[1,2,3]*, Camila Sola-Hidalgo[1,4], María Valladares[1], Orlando Astudillo[1,2] and Jorge Inostroza[1]

[1]Centro de Estudios Avanzados en Zonas Áridas (CEAZA), Coquimbo, Chile, [2]Departamento de Biología Marina, Facultad de Ciencias del Mar, Universidad Católica del Norte (UCN), Coquimbo, Chile, [3]Center for Climate and Resilience Research (CR2), Santiago Chile, [4]ONG Jáukén, Santiago, Chile

Environment imposes physiological constraints which are life-stage specific as growth-maintenance and/or growth-reproduction energetic requirements are size and volume-dependent. The scallop *Argopecten purpuratus*, one of the most important bivalve species subjected to fishery and aquaculture along the Humboldt Current System, inhabits spaces affected by continuous changes in temperature, pH, oxygen, and food availability driven by remote and local oceanographic processes. Specifically, in Chile, this species is mainly cultured in central-north Chile where is permanently affected by upwelling events of dissimilar intensity and duration which generate local conditions of acidification, deoxygenation, and cooling with different magnitudes. However, to date, it remains unknown how this economic valuable resource is physiologically affected throughout its life cycle by the continuous environmental changes driven by upwelling events of different intensities and duration along the year. Here, for the first time, *A. purpuratus* life-stage physiological sensitivity was assessed at a seasonal scale through a year-field experiment where growth, calcification, and survivorship were evaluated. Our study shows how seasonal differences in the upwelling phenology (here measured as changes in temperature, dissolved oxygen, pH, and primary productivity, but also as the number, duration, and intensity of cooling and de-oxygenation events) notably impacted the *A. purpuratus* physiological performance from juvenile to adult life-stages. This was especially noticeable during the *spring* season which showed the most intense cooling and deoxygenation events driven by stronger favorable-upwelling winds and the lowest growth and gross calcification rates (the highest decalcification rates) where adult stages showed the lowest performance. On the other hand, *A. purpuratus* survivorship was not significantly affected by upwelling intensity which would be providing evidence of the high physiological flexibility and

well-locally adapted is this species to fluctuating and occasional stressful environmental conditions. Our results are significantly relevant in the climate change context as some upwelling systems are at risk to change shortly (i.e., an upwelling intensification in frequency and intensity) as a consequence of changes in the atmospheric pressures that modulate favourable-upwelling winds. These changes may certainly increase the climate related-risks of the entire socio-ecological systems related to the fishery and aquaculture of *A. purpuratus* along the Humboldt Current System.

1 Introduction

Physiological performance is highly dependent on environmental conditions (Thomsen et al., 2015; Byrne, 2012). Elevated temperatures increase organism's metabolic rates accelerating growth and sexual maturity, while when habitat temperatures exceed the organism tolerance thresholds can promote the rapid deterioration of cellular processes (Pörtner, 2008). Also, low seawater pH values can cause hypercapnia with cascading effects on multiple physiological responses of diverse taxa, being specifically detrimental in calcifiers as shell precipitation and shell integrity are highly dependent on pH and carbonate concentration conditions (e.g., Kroeker et al., 2013; Ramajo et al., 2016; Ramajo et al., 2020). Indeed, lower pH levels result in lower calcification rates, increasing shell malformations (Waldbusser et al., 2015) and shell mechanical changes (e.g., weaker shells) (Zhao et al., 2020; Lagos et al., 2021) which also may increase the vulnerability to predation, parasitism, and/or stress by wave action (Gazeau et al., 2013; MacLeod and Poulin, 2015; Gaylord et al., 2015). Likewise, critical physiological processes such as respiration are dependent on the flux of oxygen (Seibel, 2011) where low oxygen availability is usually related to reduced growth and low reproduction success, altered behavior patterns, and increased risk of predation with resulting lower survivorship for many marine species (Breitburg et al., 2018).

Moreover, physiological sensitivity to environmental changes is life-stage specific (Talmage and Gobler, 2010; Baumann et al., 2012). Early life-stages such as larvae or juveniles usually show lower energy reserves and smaller tolerance limits making them more sensitive than adults to higher temperatures (e.g., Truebano et al., 2018), decreasing pH levels (e.g., Kroeker et al., 2013; Wessel et al., 2018), and hypoxic conditions (e.g., Clark and Gobler, 2016). Also, growth-maintenance and/or growth-reproduction *trade-offs* are more evident when organisms get older as maintenance, growth, and

reproduction related-costs are size and volume-dependent (Bayne and Newell, 1983; Kooijman, 2000; Thompson and MacDonald, 2006; Chauvaud et al., 2012). In particular, for calcifying organisms, some physiological *trade-offs* emerge as a consequence of the higher energetic requirements needed for biomineralization and calcification processes including carbonate precipitation and shell organic and periostracum production (Palmer, 1981; Trussell and Smith, 2000; Clark et al., 2020; Ramajo et al., 2019; Ramajo et al., 2020) which could represent up to 75-410% of the energy invested for growth and reproduction (Palmer, 1981).

The scallop *Argopecten purpuratus* is one of the most important bivalve species subjected to fishery and aquaculture along the Peruvian and Chilean Humboldt Current System (Yáñez et al., 2017). Historical *A. purpuratus* landings show an important variability as a consequence of changes in environmental conditions (Lagos et al., 2016; Yáñez et al., 2017) with significant impacts on Chilean and Peruvian markets (von Brand et al., 2016). Previous experimental and field studies on this resource show significant sensitivity to changes in temperature, pH, oxygen, and food availability (Lagos et al., 2016; Ramajo et al., 2016; Lardies et al., 2017; Ramajo et al., 2019; Ramajo et al., 2020; Avendaño and Cantillánez, 2022) which is particularly important in Chile as this scallop species is mostly cultured (i.e., Tongoy Bay) under the effects of one of the most active upwelling centers on the Chilean coast (Figueroa and Moffat, 2000; Rutllant and Montecino, 2002; Aravena et al., 2014; Rahn and Garreaud, 2014). Environmental conditions at Tongoy Bay have important physiological impacts on *A. purpuratus* juveniles (Ramajo et al., 2020), especially during the upwelling season (spring-summer) when the intensity and duration of upwelling events are higher (Moraga-Opazo et al., 2011; Bravo et al., 2016). However, to date, remains unknown which is the life-stage *A. purpuratus* sensitivity to changes in the environmental conditions driven by the seasonal upwelling cycle. This missing information is

significantly relevant in the climate change context as some Eastern Boundary Upwelling Systems (EBUS) are at risk to change shortly (i.e., an upwelling intensification as a consequence of changes in the frequency and intensity) which could also favor local ocean acidification and deoxygenation (see Garreaud and Muñoz, 2005; Aravena et al., 2014; Sydeman et al., 2014; Rykaczewski et al., 2015; IPCC, 2021). Certainly, potential changes in the upwelling phenology may threaten the fishery and aquaculture scallop industry and the related-socioecological system along the Humboldt Current System (Lluch-Cota et al., 2014; Bakun et al., 2015; Ramajo et al., 2020; IPCC, 2021).
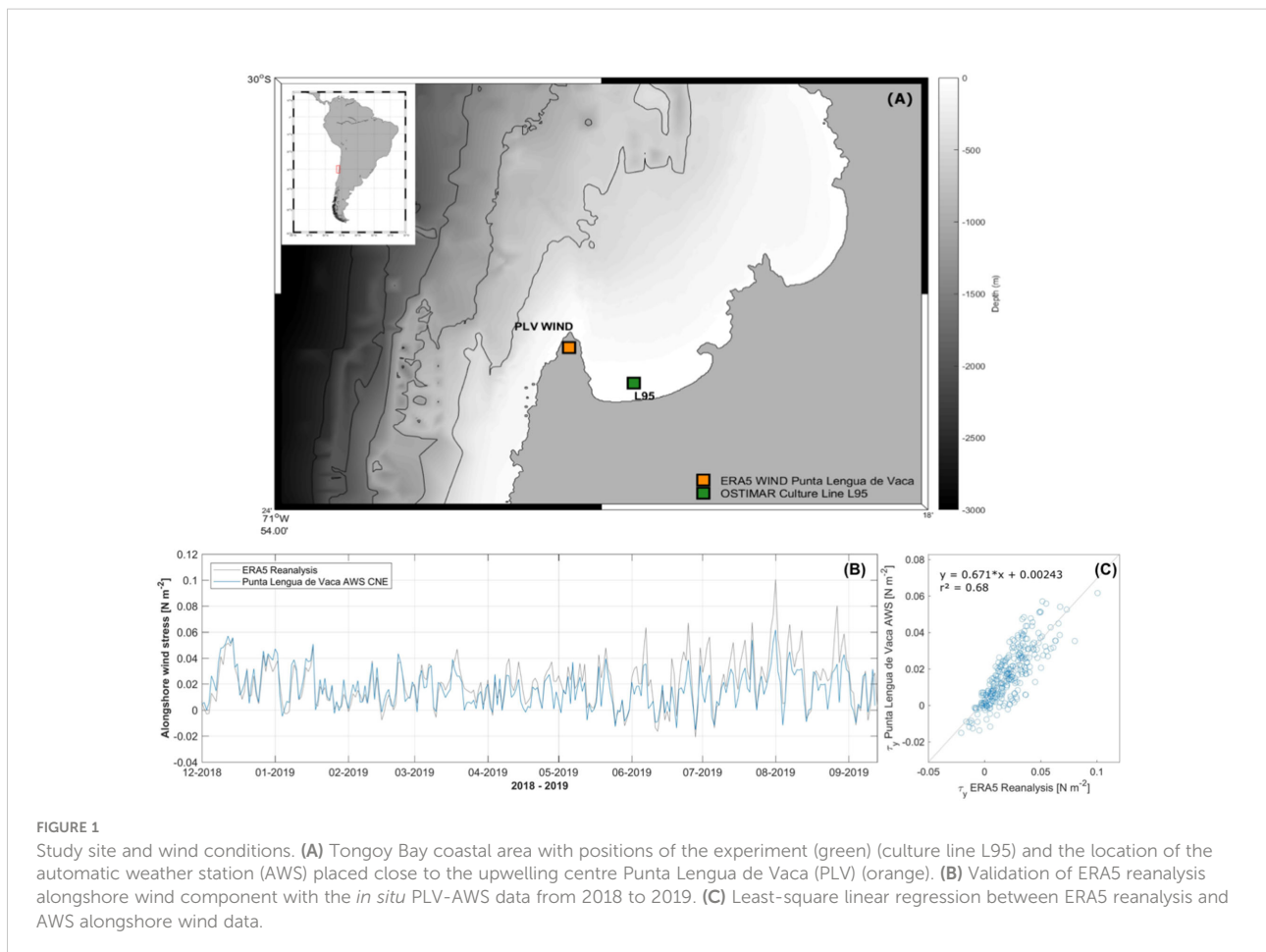
Based on that, here was assessed, for the first time, the level of physiological sensitivity of different life-stages of *A. purpuratus* at a seasonal scale in the context of upwelling. To do that, a year-field experiment was performed in Tongoy Bay where physiological responses (growth, calcification, and survivorship) were evaluated in a large range of scallop sizes (from the juvenile to adult stages) aiming to capture how seasonal changes in the upwelling phenology (number of events, duration, and intensity) could be modulating the physiological performance and fitness of this economical

valuable resource for the fishery and shellfish aquaculture along the Humboldt Current System.

2 Material and methods

2.1 Study site

Tongoy Bay, in north-central Chile, is a key place for the culture of the scallop *Argopecten purpuratus*. This bay is located just north of Punta Lengua de Vaca (PLV), one of the most important and active upwelling centers that modulate environmental conditions on the central-north Chilean coast (Figueroa and Moffat, 2000; Rutllant and Montecino, 2002; Rahn and Garreaud, 2014) (Figure 1A). Previous studies have determined that Tongoy Bay shows a semi-permanent upwelling regime with higher upwelling intensities during the austral spring-summer seasons (Moraga-Opazo et al., 2011; Bravo et al., 2016). By the year, seasonal differences in the upwelling phenology provoke important oceanographic, biogeochemical, and environmental heterogeneity in the

FIGURE 1
Study site and wind conditions. **(A)** Tongoy Bay coastal area with positions of the experiment (green) (culture line L95) and the location of the automatic weather station (AWS) placed close to the upwelling centre Punta Lengua de Vaca (PLV) (orange). **(B)** Validation of ERA5 reanalysis alongshore wind component with the *in situ* PLV-AWS data from 2018 to 2019. **(C)** Least-square linear regression between ERA5 reanalysis and AWS alongshore wind data.

nearby coastal areas (Torres et al., 1999; Torres and Ampuero, 2009; Ramajo et al., 2020). As a consequence of this seasonal pattern and upwelling, Tongoy Bay shows along the year high fluctuations in terms of temperature (10.6°C - 19.7°C), pH (7.6 - 8.1), oxygen concentrations (1.45 - 4.17 ml L^{-1}) (Ramajo et al., 2019; Ramajo et al., 2020), and primary productivity (ranging from 2.40 to 10.45 mg m^{-3}) (Rutllant and Montecino, 2002; Ramajo et al., 2020).

2.2 Organismal collection and experimental design

Wild scallops from Tongoy Bay (30°16'S; 71°35'W), with no shell damage and parasite presence (Basilio et al., 1995), were provided by the scallop aquaculture company OSTIMAR S.A. The experimental design consisted of four analogous field experiments (hereafter, *seasonal experiments*) that aimed to determine how seasonal environmental changes are modulated by upwelling phenological changes (i.e. a semi-permanent upwelling regime with lower intensity during the autumn and winter months, and higher intensity during spring-summer seasons, Thiel et al., 2007; Torres and Ampuero, 2009; Rahn and Garreaud, 2014) and may be affecting different life-stages (from juveniles to adults) of the scallop *A. purpuratus* at Tongoy Bay. To do that, around 180 scallops were used in each *seasonal*

experiment with a body-size range between 10 to 90 mm (Figure S1). After collection, experimental scallops were transported under-insulated conditions to the laboratory and labeled with numbered tags glued onto the shells allowing their identification during the experiment. After that, between 100 - 120 scallops (hereafter, *alive scallops*) were maintained in aquaria under controlled conditions (14°C, pH$_{NBS}$ near 8.0, and >90% of oxygen saturation). In addition, ~ 60 scallops were sacrificed and their soft parts were removed, and shells were kept for the experiment (hereafter, *empty shells*). For both, *alive scallops* and *empty shells*, the maximum shell size (length and width), and the shell buoyant weight were recorded at the initial time (Figure S1). After that, *alive scallops* and *empty shells* were randomly distributed in 4 *pearl nets* (i.e. common culture structures used by the aquaculture industry to avoid denso-dependency issues). Each *pearl net* was composed of 2 different nets separated by less than 25 cm between them. Each *pearl net* contained 30 *alive scallops* and 30 *empty shells* (see Figure 2). The four experimental *pearl nets* were located in the culture line number L95 belonging to OSTIMAR S.A (30°16'49.4''S; 71°34'03.7''W) (Figure 1A) at 9 m depth. Each *alive scallop* and each *empty shell* were considered independent replicates. The four *seasonal experiments* followed similar experimental protocols. The *Summer* experiment was carried out between January to March 2019, the *Autumn* experiment between March to July 2019, *Winter* from July to October 2019, and the *Spring* experiment from October 2019 to
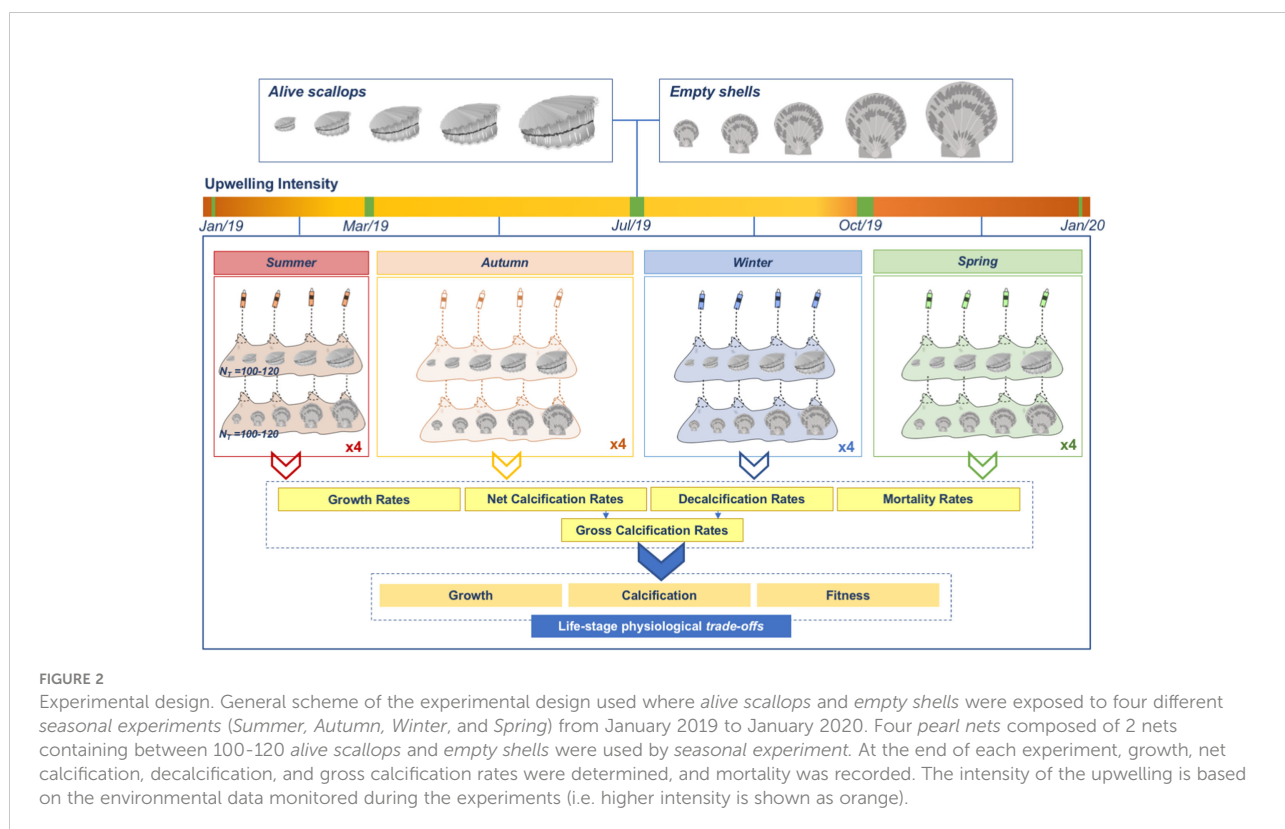
FIGURE 2
Experimental design. General scheme of the experimental design used where *alive scallops* and *empty shells* were exposed to four different *seasonal experiments* (*Summer, Autumn, Winter*, and *Spring*) from January 2019 to January 2020. Four *pearl nets* composed of 2 nets containing between 100-120 *alive scallops* and *empty shells* were used by *seasonal experiment*. At the end of each experiment, growth, net calcification, decalcification, and gross calcification rates were determined, and mortality was recorded. The intensity of the upwelling is based on the environmental data monitored during the experiments (i.e. higher intensity is shown as orange).

January 2020 (see Figure 2). At the end of each *seasonal experiment*, *pearl nets* with *alive scallops* and *empty shells* were removed from the L95 and transported to the laboratory where shell size (maximum length and width) and buoyant weight were measured. At the end of each *seasonal experiment*, all *alive scallops* were sacrificed (not returned to the field).

2.3 Environmental conditions at Tongoy Bay

Tongoy Bay environmental conditions, at high and low frequencies, were monitored during the four *seasonal experiments*. High-frequency (each 15 min) temperature and dissolved oxygen (DO) conditions were registered by using HOBO U26 Dissolved Oxygen Data Loggers (ONSET[®]) which were attached to the experimental *pearl nets*. According to the manufacturer's instructions, every six months the oxygen logger membranes were replaced with new ones. Anti-fouling sensor maintenance, as well as, data downloading from each sensor were performed at the end of each *seasonal experiment*. At low frequency (weekly), pH_{NBS} conditions were determined by collecting water samples through a NISKIN bottle (5 L vol). Three water samples per depth were analyzed within 60 min after water collection using a Metrohm 780 Meter (Metrohm[®]) connected to a combined electrode (Aquatrode Plus with Pt1000, Metrohm[®]). The electrode was calibrated using three NBS buffers (Metrohm[®]) at 25°C before each measurement. In addition, surface chlorophyll-*a* (Chl-*a*) by each *seasonal experiment* was obtained through 8-day composites of Moderate Resolution Imaging Spectroradiometer (MODIS-Aqua) 4km products retrieved from NASA (http://oceancolor.gsfc.nasa.gov) comprising an area limited by 30.6° - 30°S and 71.9°W to the coast. MODIS Chl-*a* data were averaged at a monthly scale and then averaged for each *seasonal experiment*. Finally, the intensity and variability of wind-driven coastal upwelling were obtained from ERA5 reanalysis (https://rda.ucar.edu/datasets/ds633.0/) at PLV during the experiment. PLV is representative of the environmental conditions occurring at Tongoy Bay as it was recently observed by Ramajo et al. (2020) (see also Figure 1A). Reanalysis dataset was validated against available continuous 10m wind data from an Automatic Weather Station (AWS) at the same geographic location between December 2018 to September 2019 (see Figure 1B). Daily alongshore wind magnitude measured by the AWS at PLV and ERA5 reanalysis showed a high and significant correlation (*Pearson* correlation: R^2 = 0.68, *P*-value = 0.000) (see Figure 1C).

2.4 Growth, calcification, and mortality

Growth rates (GR), net calcification rates (NCRs), decalcification rates (DCRs), and gross calcification rates (GCR) were estimated for all *seasonal experiments*. GRs estimations

correspond to the difference in the total area of *alive scallops* (estimated as an ellipsoid from shell maximum length and width measurements) divided by the number of days that the experiment lasted. *Empty shells* were used to estimate size differences in DCRs for each *seasonal experiment* (see Figure S2). Previous studies have found that low pH conditions generate corrosive and undersaturated carbonate conditions which are responsible for shell layers dissolution and higher decalcification rates (i.e., Waldbusser et al., 2011; Langer et al., 2014). Both NCRs and DCRs were estimated by using the buoyant weight technique (Davies, 1989). Buoyant weight data was converted into shell dry weight (DW) using the seawater density (average conditions at Tongoy Bay, salinity = 34‰, temperature = 14°C), and the density of calcite (2.71 g cm^{-3}) (see Ramajo et al., 2019). Finally, NCRs and DCRs were computed as the change in the shell dry (DW) weight goes by between two different periods (i.e. duration of each *seasonal experiment*). Lastly, GCRs for each *alive scallop* and *seasonal experiment* were determined by subtracting DCRs from the NCRs. All physiological rates (i.e. GRs, NCR, DCRs, and GCRs) are shown as non-normalized and body-size normalized. Dead organisms were counted at the end of each *seasonal experiment*, and mortality rates were estimated as the percentage of dead organisms per day (% d^{-1}).

2.5 Data analyses

Environmental and biogeochemical seawater properties (i.e. pH_{NBS}, temperature and DO), based on the mean state (± standard error, SE) and their variability (coefficient of variation, CV) were established for the four *seasonal experiments*.

Upwelling was characterized by calculating alongshore wind stress ($\tau_{alongshore}$) after rotating ERA5 daily wind vectors to align them approximately with the direction of the coast (Equation 1).

$$\tau_{alongshore} = \rho_a \times C_d \times |v|v \qquad \text{Eq. (1)}$$

where ρ_{air} is air density (assumed constant at 1.22 kg m^{-3}), C_d is the drag coefficient varying with v, and v is the meridional alongshore wind component.

Further, across-shelf Ekman transport (M, units = m^2 s^{-1} per meter of the coast) was computed following:

$$M = \frac{1}{\rho_w f} \tau_{alongshore} \qquad \text{Eq. (2)}$$

where ρ_w is the water density (assumed constant at 1024 kg m^{-3}), f is the Coriolis parameter (s^{-1}), and τ is the alongshore wind stress. Positive values of M indicate onshore transport due to downwelling favorable winds, while negative values imply offshore transport caused by upwelling favorable winds (Bakun, 1975). Posteriorly, following Tapia et al. (2009) and Ramajo et al. (2020) methodologies, the impact of upwelling on temperature changes (i.e. cooling) and DO conditions (i.e. deoxygenation) at Tongoy Bay were estimated.

The present study spans one entire year in a semi-permanent upwelling region encompassing upwelling, downwelling favorable winds, and relaxation periods (Rahn and Garreaud, 2014), some extra methodological modifications to Ramajo et al. (2020) were implemented to properly attribute cooling and de-oxygenating events to upwelling. To do that, first, we defined a threshold of alongshore wind stress of 5m s^{-1} in the equatorward direction (see Cury and Roy, 1989; García-Reyes et al., 2014). Secondly, to highlight the synoptic variability dominance in upwelling systems (Renault et al., 2009), a 30-day running mean was subtracted from the daily average time series of seawater temperature and DO. Daily anomalies in temperature and DO time series were used to quantify the number, duration, and intensity of the different cooling and de-oxygenations episodes recorded during each *seasonal experiment* (Figure 5A) (for further details, see Ramajo et al., 2020).

Average specific differences in GRs, NCRs, DRs, and GCRs (non- and body-size normalized), as well as, the size distribution of alive and dead scallops after each *seasonal experiment* were evaluated by using Kruskal Wallis and Dunn tests. The role of the tested factors (*Size* and *Season*) for all physiological rates was addressed by using hierarchical linear mixed-effects models (e.g., Ramajo et al., 2020). *Size* and *Season* and the two-way interaction between these were modeled as fixed effects. Random effects at the individual level were employed to control for potential organismal effects. Restricted maximum likelihood (REML) was used to fit the model for each physiological rate (GRs, NCRs, DRs, and GCRs), as well as, to calculate unbiased estimates of parameter variance and standard error according to the general model:

$$y = Xb + X0 + Za + e$$

where y is the vector of the observations (i.e., physiological rates), b and 0 is the vector of fixed effects (i.e., *Size* and *Season*), a is the vector of random effects (i.e., individuals), *e* represents the residual effects, and X and Z are the corresponding incidence matrices. Linear mixed-effects models were estimated by using the *lme4* package. The *AFEX package* was used to obtain parameter *P*-values for the linear mixed-effects models using the Kenward-Roger approximation for degrees of freedom. Optimal models were identified as those yielding the greatest number of significant (P< 0.05) fixed effects. Variance and standard deviation of the random effect (individual) are also reported. Differences in mortality (i.e. number of dead scallops) were determined by using Poisson regressions. Finally, to identify potential associations between environmental variables and physiological rates measured, Pearson correlation analyses were carried out, and multivariate comparisons between all physiological rates and environmental variables were assessed using redundancy analysis (RDA). Before RDA analyses, environmental variables and physiological rates were standardized (from zero to one). RDA analysis was carried out using the vegan package. All these analyses were carried out on R software (version 3.5.0).

3 Results

3.1 Seasonal environmental variability at Tongoy Bay

During 2019 at Tongoy Bay, coastal upwelling conditions (i.e. negative Ekman transport, M) dominated the year-round experimental study showing an increasing intensity from summer towards the *spring* season (observed in mean and minimum values) exhibiting a maximum mean of -0.43 m^2 s^{-1} in the *winter* season. On the other hand, downwelling favorable conditions (i.e., positive Ekman transport, M) were mostly observed during the *autumn* season. Regarding upwelling relaxation events (i.e., Ekman transport close to zero), these were observed throughout the year on a synoptic time scale (~1 to 16 days) (Figure 3A; Table 1).
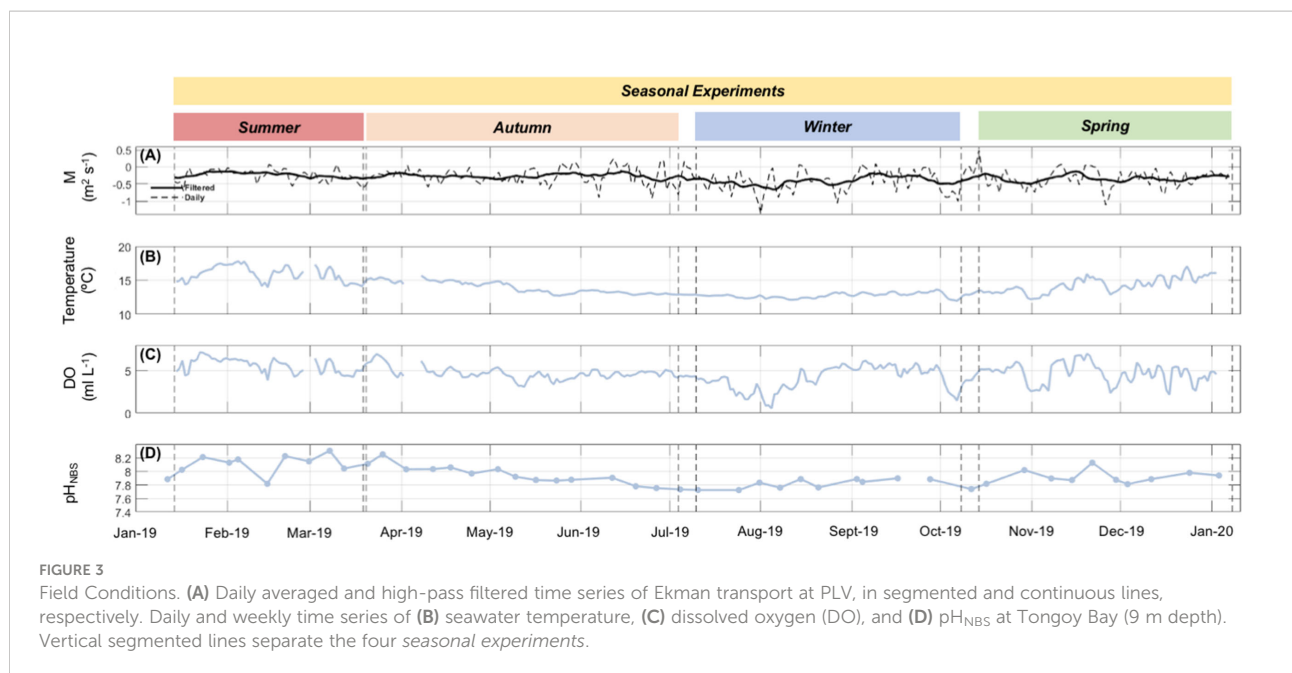
Surface Chl-*a* at Tongoy Bay presented maximum values during the *spring* and the lowest concentrations during the *autumn* and *winter* months (Figure 4; Figure S3).

In terms of variability (here measured as CV, %), temperature and pH exhibited a decline towards *winter* with a subsequent rise in *spring*. Maximum variability in temperature and pH was found during *spring and summer*, with temperature CV peaking in spring and pH CV in summer (Figures 3B, D; Table 1). DO variability increased from *summer* to *spring*, with a maximum in *winter* (Figure 3C; Table 1).

The number and duration of cooling and de-oxygenation events showed differences among *seasonal experiments* and were highly correlated with Ekman transport magnitude ((Figures 5B–D)) revealing a negative relationship between M and temperature and DO conditions (Figures 3A–D). A slight increase in the number and duration of cooling and de-oxygenation events was observed from *summer* to *winter* then showing a little reduction during the *spring* season. *Winter* presented the highest number of cooling and de-oxygenation events, as well as, the longest duration compared with the rest of the *seasons*. However, *spring* and *summer* exhibited the highest intensity and cooling and de-oxygenation rates (Figures 5E–H).

3.2 Growth and calcification

Both, average non-body-size normalized and body-size normalized GRs showed significant differences among the different *seasonal experiments* (Kruskal-Wallis test: $\chi^2 = 24.86$, *P*-value< 0.001, and $\chi^2 = 50.58$, *P*-value = 0.000, respectively). Average GRs (non-body-size normalized) showed similar values between the *summer*, *autumn*, and *winter* seasons (*Dunn's test*: *P*-value = 1.000), however a significant reduction in the GRs was detected during the *spring* in comparison with *summer* (*Dunn's test*: *P*-value = 0.000), *autumn* (*Dunn's test*: *P*-value = 0.000) and *winter* (*Dunn's test*: P-value< 0.001) (see Figure 6A). On the other hand, average normalized body-size GRs showed a different trend with a visible

FIGURE 3

Field Conditions. **(A)** Daily averaged and high-pass filtered time series of Ekman transport at PLV, in segmented and continuous lines, respectively. Daily and weekly time series of **(B)** seawater temperature, **(C)** dissolved oxygen (DO), and **(D)** pH_{NBS} at Tongoy Bay (9 m depth). Vertical segmented lines separate the four *seasonal experiments*.

decreasing trend from the *summer* to the *spring*. Normalized body-size GRs were significantly higher during the *summer* in comparison with the *winter* (*Dunn's test*: *P*-value = 0.001) and *spring* seasons (*P*-value = 0.000). No significant differences were found between *summer* and *autumn* (*P*-value = 0.080), as well as between *autumn* and *winter* (*Dunn's test*: *P*-value = 0.844) (see Figure 6B). Linear mixed models controlled for the random effects of individuals confirmed that the scallops' size (*P*-value< 0.001),

TABLE 1 Tongoy Bay environmental conditions.

Environmental Varisable	Seasonal Experiments (Jan 2019 – Jan 2020)			
	Summer (Jan – Mar)	Autumn (Mar – Jul)	Winter (Jul – Oct)	Spring (Oct – Jan)
Ekman Transport (M) (m^2 s^{-1})				
Mean (± SE)	-0.23 ± 0.02	-0.26 ± 0.02	-0.43 ± 0.03	-0.33 ± 0.03
Max - Min	0.08 – -0.71	0.25 – -0.92	0.10 – -1.38	0.51 – -1.12
Temperature (° C)				
Mean (± SE)	15.93 ± 0.14	13.90 ± 0.08	12.76 ± 0.04	14.31 ± 0.12
Max - Min	17.79 – 13.98	15.67 – 12.73	13.66 – 11.97	17.04 – 12.22
CV (%)	7.04	6.21	2.9	7.85
Dissolved Oxygen (DO) (ml L^{-1})				
Mean (± SE)	5.61 ± 0.10	4.68 ± 0.07	4.06 ± 0.15	4.70 ± 0.13
Max - Min	7.16 – 3.88	6.96 – 3.10	6.18 – 0.55	6.99 – 2.16
CV (%)	14.86	15.08	35.24	25.61
pH$_{NBS}$ (25° C)				
Mean (± SE)	8.117 ± 0.048	7.959 ± 0.036	7.818 ± 0.021	7.919 ± 0.031
Max - Min	8.301 – 7.814	8.249 – 7.751	7.895 – 7.722	8.125 – 7.809
CV (%)	1.77	1.7	0.91	1.23

Ekman transport (M), temperature, dissolved oxygen (DO), and pH$_{NBS}$ were recorded during the different seasonal experiments at Tongoy Bay. Variability for each variable was estimated by the Coefficient of Variation (CV, %).
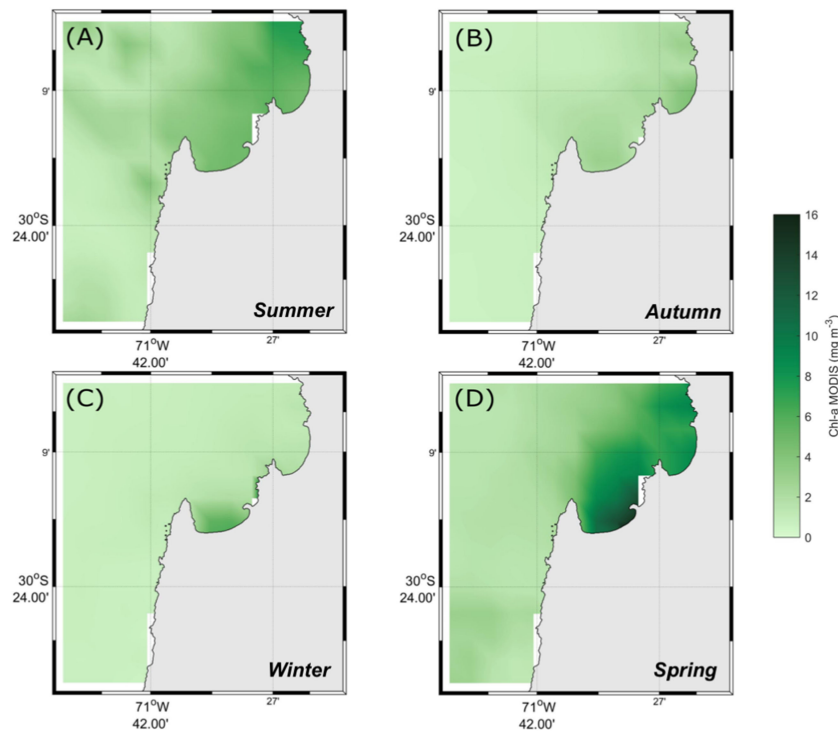
FIGURE 4
Chlorophyll-*a* variability. Seasonally-averaged Chl-*a* fields derived from MODIS-Aqua 8-day composites for each *seasonal experiment.*. **(A)** Summer, **(B)** Autumn, **(C)** Winter, and **(D)** Spring season.

season (i.e., the environmental conditions occurring during each *seasonal experiment)* (P-value< 0.037), and the interaction between size and *season* (P-value = 0.030) predicted significantly the GRs observed (Figure 7A; Table 2).

Both average NCR (non-normalized and normalized body-size) showed significant differences among the different *seasonal experiments* (*Kruskal-Wallis's test*: $\chi2 = 13.17$, P-value = 0.004, and $\chi2 = 29.77$, P-value = 0.000, respectively). Non-normalized body-size NCRs did not show a clear pattern along the year-round experiment showing similar values during the *autumn* (Dunn test: P-value = 1.000), *winter* (*Dunn's test*: P-value = 1.000), and *spring* (*Dunn's test*: P-value = 1.000) However, non-normalized body-size NCRs were significantly lower in *summer* in comparison with *autumn* (*Dunn's test*: P-value = 0.011), and *winter* (*Dunn's test*: P-value = 0.0120) (see Figure 6C). On the other hand, normalized body-size NCRs showed a clear pattern with decreasing values from *summer* to *spring* (Figure 6D), presenting significant lower values during *spring* in comparison with *autumn* (*Dunn's test*: P-value< 0.001) and *winter* (*Dunn's test*: P-value< 0.001). Normalized body-size NCRs were also higher during *summer* in comparison with *winter* (*Dunn's test*: P-value = 0.016). No significant differences were found between *autumn* and *summer* (Dunn test: P-value = 1.000) and *winter* (*Dunn's test*: P-value = 0.330), as well as between *winter* and *spring* (*Dunn's test*: P-value = 0.054) (see Figure 6D).

Linear mixed models controlled for the random effects of individuals confirmed that both seasons (i.e., environmental conditions occurring at each *seasonal experiment*) and *size* factors predicted significantly the NCRs observed (*Size* x *Season*; P-value= 0.002) (Figure 7; Table 2).

DRs in *alive scallops* (non-body-size and normalized body-size) showed significant differences among the *seasonal experiments* (*Kruskal-Wallis's test*: $\chi2 = 211.58$, P-value = 0.000, and $\chi2 = 211.11$, P-value = 0.000, respectively), being significantly higher during the *spring* (see Figures 6E, F). Linear mixed models controlled for the random effects of individuals confirmed that the interaction between *size* and season factors predicted significantly the DRs observed (P-value< 0.011) (see Figure 7; Table 2).

Both, non- and normalized body-size GCRs were significantly different among the different *seasonal experiments* (*Kruskal-Wallis's test*: $\chi2 = 102.07$, P-value = 0.000, and $\chi2 = 93.96$, P-value = 0.000, respectively). *Spring* season showed the lowest GCRs in comparison with *summer*, *autumn*, and *winter* seasons in both non-normalized (Dunn test: P-value = 0.000) and normalized body-size GCRs (*Dunn`s test*: $P$-value = 0.000) (Figures 6G, H). GCRs (non-normalized and normalized body-size) did not show significant differences between the *autumn*, *winter*, and *summer* seasons (*Dunn`s tests*: P-value< 0.05 for all combinations). Linear mixed models controlled for the random effects of individuals confirmed
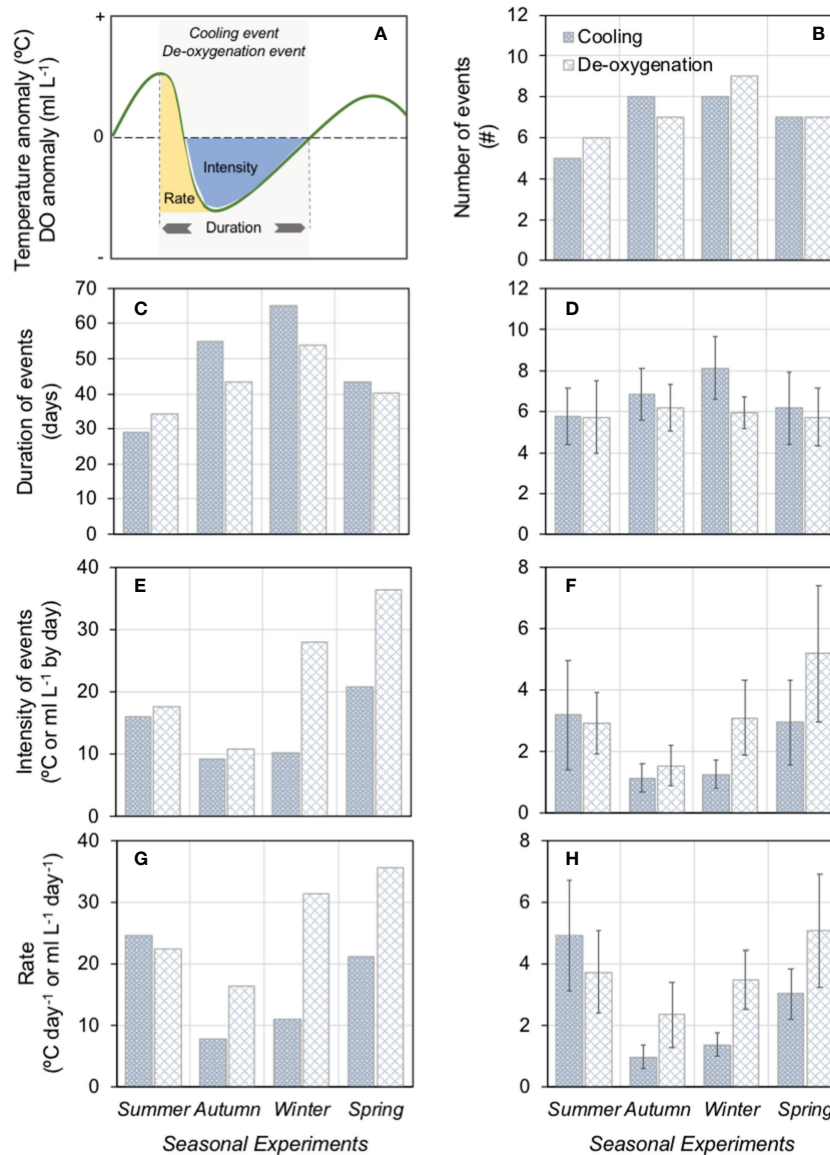
FIGURE 5

Cooling and de-oxygenation at Tongoy Bay. **(A)** Scheme of the methodology used to determine the upwelling impact on cooling and de-oxygenation events based on thermal and dissolved oxygen anomalies (see section 2.1 for further details). Number **(B)**; accumulated **(C)** and mean **(D)** duration; accumulated **(E)** and mean **(F)** intensity (as an integrated anomaly); accumulated **(G)** and mean **(H)** rate (as integrated cooling/deoxygenation) of events registered each *seasonal experiment*. Data in D, F, and H are means $\pm$ SE.

that *size* (*P*-value< 0.001), *season* (i.e., the environmental conditions occurring during each *seasonal experiment*) (*P*-value = 0.023), and the interaction between *size* and *season* factors (*P*-value = 0.001) predicted significantly the GCRs observed (Figure 7; Table 2).

3.3 Mortality

Higher mortality rates were found during the *spring* and *summer* seasons which corresponded to the 57% and 35% of

initial experimental scallops used for each *seasonal experiment*, respectively. On average, dead scallops in *summer* and *spring* seasons mortalities occurred in those organisms with larger sizes (88.65 and 92.97 mm maximum shell length, respectively) (see Figure 8A). However, mortality rates (Poisson regression: $\chi2 = 4.3825$, *P*-value = 0.223) and size of the dead scallops (Kruskal-Wallis test: $\chi2 = 7.6931$, *P*-value = 0.053) did not show any significant difference among the *seasonal experiments* (Figure 8B).
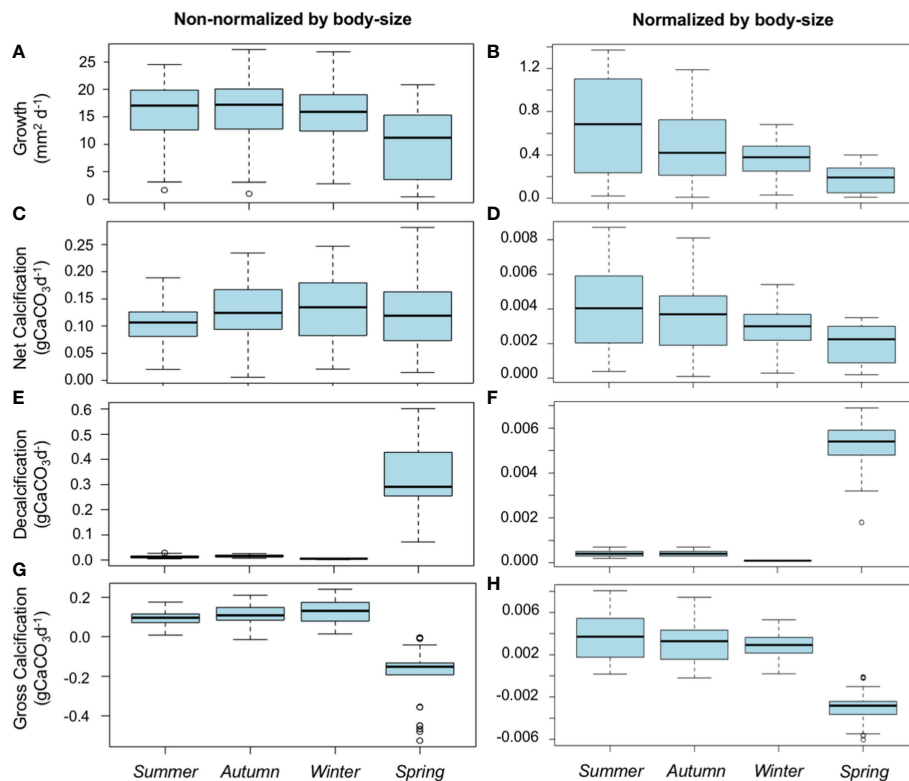
A. purpuratus **physiological rates**. Average non-normalized and normalized body-size growth **(A, B)**, net calcification **(C, D)**, decalcification **(E, F)**, and gross calcification rates **(G, H)** were recorded during the four *seasonal experiments*. Data shown are mean ± SE.

3.4 Interaction between environmental conditions and scallop physiology

High collinearity between environmental conditions recorded at each *seasonal experiment* and physiological *A. purpuratus* performance was corroborated by the RDA analyses (Figure 9A). The two main components explained, in total, more than 99% of the observed variance (89.8% of Component RDA1 and 9.96% of Component RDA2). Ekman transport, pH, DO and temperature were all highly correlated (RDA2), while Chl-*a* showed a higher load along the RDA1 axis, and thus, a lower correlation with the variables previously mentioned (Figure 9A).

In particular, strong negative and significant correlations were found between Ekman transport and the temperature, DO, and pH levels of Tongoy Bay. On the other hand, pH and DO showed stronger positive and significant correlations. Weak correlation values were observed (positive and significant) between temperature and pH and DO. Chl-*a* showed a positive and significant correlation with Ekman transport, as well as a negative and significant correlation with DO and pH values.
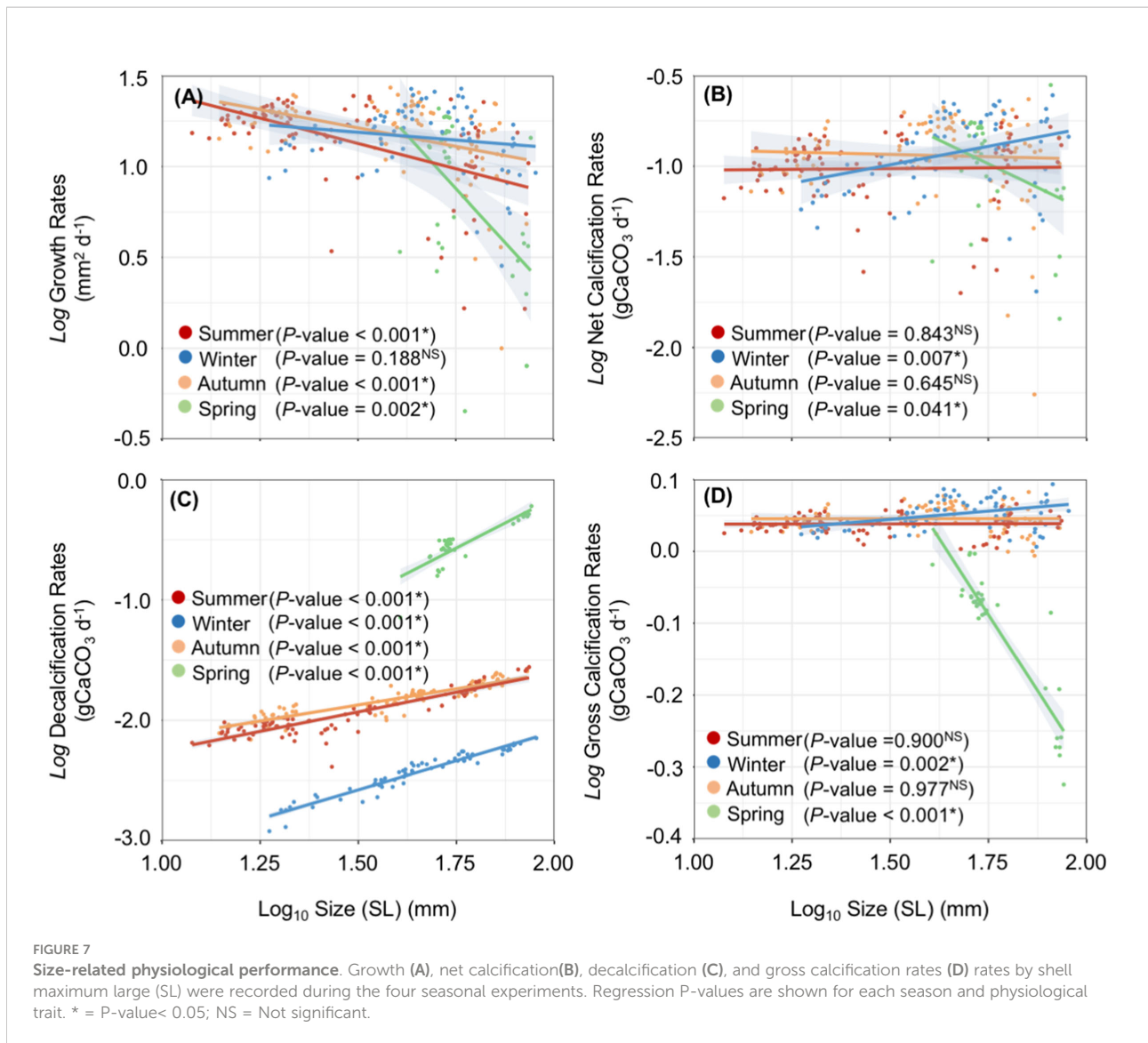
Related to physiological responses, GRs showed a positive and significant correlation with NCR and GCRs, and a negative and significant correlation with DRs. NCRs showed a negative and

significant correlation with DRs, and a positive and significant correlation with GCRs. GCRs and DCs showed a significant and strong negative correlation

Finally, strong correlations were found between the environmental variables (Ekman transport, temperature, DO, pH, and Chl-*a*) and *A. purpuratus* physiological responses (GRs, NCRs, DCs, and GCRs) (Figure 9B). GRs and NCRs showed significant positive correlations with DO and pH, while this correlation was negative with Ekman transport and Chl-*a*, and null with temperature. DRs showed significant and positive correlations with temperature and Chl-*a* values, however, no significant correlations were observed between DRs with DO, pH, and Ekman transport. GCRs showed a negative significant correlation with Ekman transport, temperature, and Chl-*a* values, and positive with pH values.

4 Discussion

Marine environmental conditions are modulated by remote and local drivers that alter, at multiple spatiotemporal scales, several physical, chemical, biological and socio-ecological processes (e.g., Bakun et al., 2015; Sprogis et al., 2018). Environmental fluctuations have important effects on the physiological performance of marine

Size-related physiological performance. Growth **(A)**, net calcification**(B)**, decalcification **(C)**, and gross calcification rates **(D)** rates by shell maximum large (SL) were recorded during the four seasonal experiments. Regression P-values are shown for each season and physiological trait. * = P-value< 0.05; NS = Not significant.

organisms with significant consequences on the ecosystem structure and functioning, as well as, on the state of the socio-ecological systems (SES) related to fisheries or aquaculture (Sprogis et al., 2018; Bertrand et al., 2020). Our study shows the major role of upwelling shaping the annual physiological performance and fitness of the scallop *A. purpuratus*, one of the most important resources subjected to fishery and aquaculture along the Humboldt Current System.

Tongoy Bay, in central-north Chile, is the main location where the scallop *A. purpuratus* is cultured in Chile. This area is permanently affected by changes in seawater temperature, dissolved oxygen, pH, and primary productivity as a consequence of the upwelling transport forced by coastal wind patterns (e.g., Ramajo et al., 2020). The magnitude of environmental changes is modulated by the seasonal and intra-seasonal variability of the local atmospheric forcing controlling the phenological upwelling pattern (i.e., number, intensity, and duration of upwelling, relaxation, and

downwelling events). Seasonal differences in upwelling phenology (here measured as changes in temperature, oxygen pH, and primary productivity, but also as the number, duration, and intensity of cooling and de-oxygenation events) affected the physiological performance and fitness of the different *A. purpuratus* life-stages tested. *Spring* and *summer* experimental periods showed higher intensities of cooling and deoxygenation events which, on average, produced lower growth and gross calcification rates (higher decalcification rates), especially in *A. purpuratus* adults. On the other hand, although higher mortalities were recorded under more intense upwelling periods (*spring* and *summer)*, environmental conditions driven by upwelling did not significantly affect the *A. purpuratus* survivorship confirming the high physiological flexibility and well-locally-adaptation of this species to the fluctuating and stressful environmental conditions imposed by upwelling (Lagos et al., 2016; Ramajo et al., 2016; Ramajo et al., 2020).
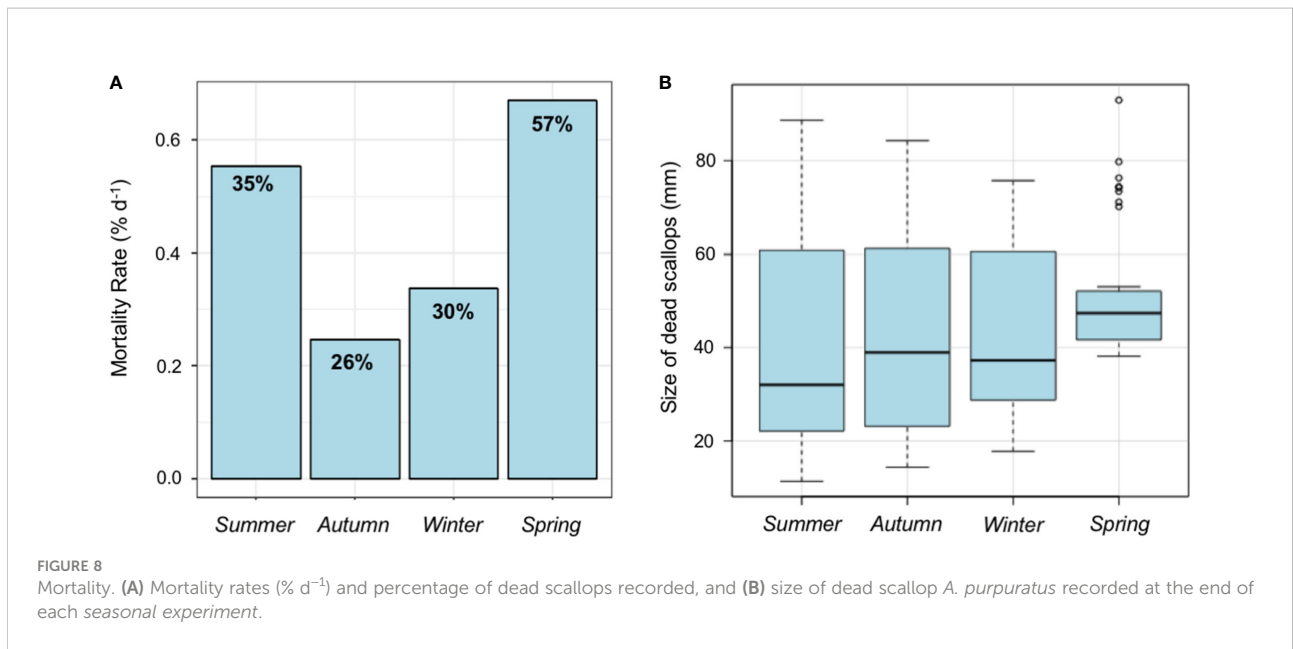
TABLE 2   Growth and Calcification.

Fixed Effects	Estimates	CI	P-value
Growth Rate (mm^2 d^{-1})			
Intercept	25.05	21.36 – 28.74	**<0.001**
Size	-0.21	-0.29 – -0.14	**<0.001**
Season	-1.43	-2.78 – -0.09	**0.037**
Size × Season	0.03	0.00 – 0.06	**0.030**
Random Effects	**Variance**	**SD**	
Individual	5.20	2.28	
Net Calcification Rate (gCaCO$_3$ d^{-1})			
Intercept	0.15	0.12 – 1.01	**<0.001**
Size	0.00	-0.00 – 0.00	0.071
Season	-0.02	-0.03 – -0.01	**0.004**
Size × Season	0.00	0.00 – 0.00	**0.002**
Random Effects	**Variance**	**SD**	
Individual	0.00	0.00	
Decalcification Rate (gCaCO$_3$ d^{-1})			
Intercept	-0.08	-0.15 – -0.01	**0.027**
Size	0.00	0.00 – -0.01	**<0.001**
Season	0.02	-0.01 – 0.04	0.225
Size × Season	0.00	-0.00 – -0.00	**0.011**
Random Effects	**Variance**	**SD**	
Individual	0.00	0.00	
Gross Calcification Rate (gCaCO$_3$ d^{-1})			
Intercept	0.23	0.15 – 0.31	**<0.001**
Size	0.00	-0.01 – 0.00	**<0.001**
Season	-0.03	-0.06 – -0.00	**0.023**
Size × Season	0.00	0.00 – 0.00	**0.001**
Random Effects	**Variance**	**SD**	
Individual	0.00	0.00	

Summary of statistical parameters for linear mixed-effects models for growth rates, net calcification rates, decalcification rates, and gross calcification rates. Relative variance of the random effects (individual) is shown. Bold texts show significant P-values at α = 0.05.

It is known that upwelling, forced by the alongshore southerly favourable-winds, provokes a replacement of surface seawater by deeper water masses (Chapman, 1996; Bravo et al., 2016) which are colder, richer in nutrients and pCO$_2$ (low pH), and poor in oxygen concentrations (Huyer, 1983; Garcia-Reyes et al., 2015, Ramajo et al., 2020; Kämpf and Chapman, 2016). Alongshore upwelling-favourable winds at PLV (nearest upwelling center to Tongoy Bay) had significant effects on Tongoy Bay's environmental and biogeochemical conditions during the experiment, where the highest strength of upwelling (i.e., more negative Ekman transport
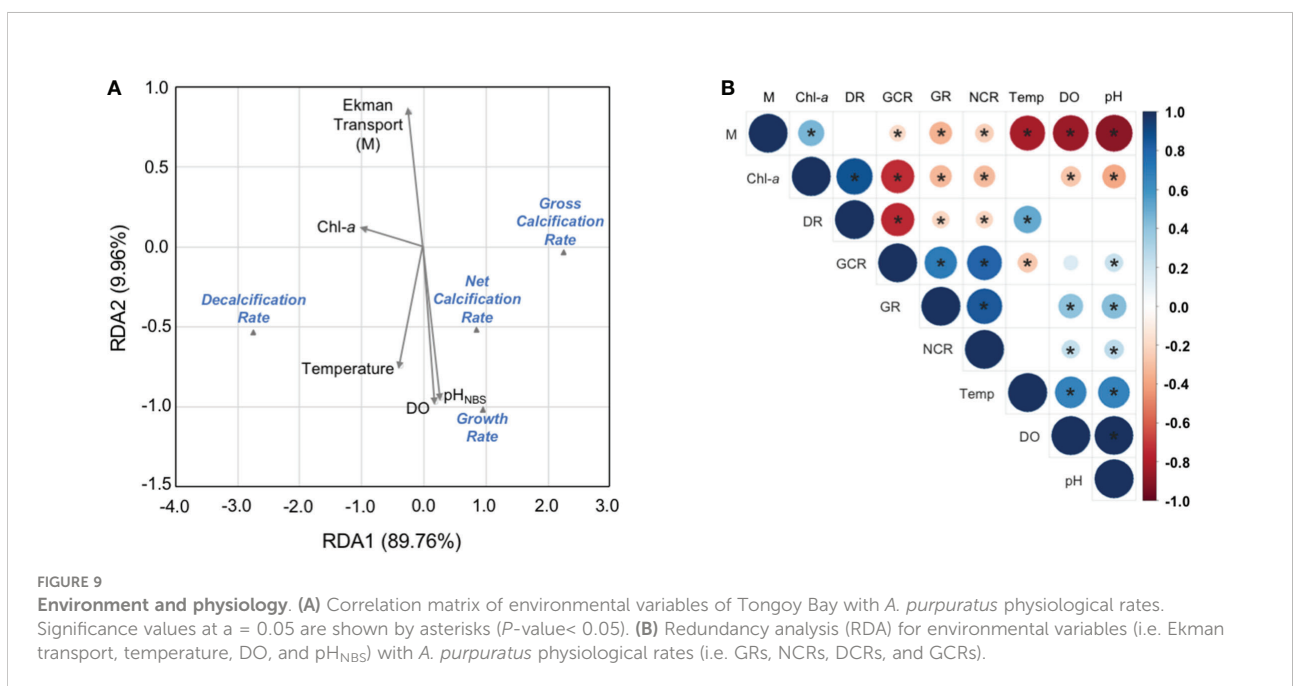
values) occurred during the *winter* and *spring* months. Environmental conditions recorded during 2019-2020 partially agrees with previous studies that show year-round upwelling activity, peaking during the spring season at 30°S (Strub et al., 1998; Torres et al., 1999; Rutllant and Montecino, 2002; Torres and Ampuero, 2009; Aravena et al., 2014; Rahn and Garreaud, 2014). However, climate change is forcing shifts in major atmospheric high-pressure Hadley cells that trigger an intensification and a change of the intraseasonal variability of the alongshore favourable-upwelling winds (Lu et al., 2007; Rykaczewski et al., 2015; Schneider et al., 2017)

FIGURE 8
Mortality. **(A)** Mortality rates (% d^{-1}) and percentage of dead scallops recorded, and **(B)** size of dead scallop *A. purpuratus* recorded at the end of each *seasonal experiment*.

particularly, in the poleward part of the Humbolt Current System (e.g., Aguirre et al., 2018; Aguirre et al., 2021; Belmadani et al., 2014) which may be explaining why intense upwelling events occurred during the *winter* season.

Major Ekman transport values (M) were significantly correlated with lower seawater temperatures, DO and pH values, and higher Chl-*a* concentrations similar to those recently observed at Tongoy Bay by Ramajo et al. (2020). Annual seawater temperature pattern followed the solar radiation annual cycle with higher mean values recorded in *summer* and *spring*, and lower in *winter* months.

However, the *summer* and *spring* months presented higher temperature variability with values ranging between 12-13°C to 18°C. Higher temperature values can be explained by the higher solar radiation occurring during the *summer* and *spring* months, while lower temperatures can be attributed to the higher cooling rates associated with upwelling events of higher intensity observed at Tongoy Bay. The lowest dissolved oxygen and pH average values were recorded in the *winter* months when Ekman transport values were higher. *Winter* and *spring* months showed a high number of deoxygenation events with higher duration and intensity. Moreover, the

FIGURE 9
Environment and physiology. **(A)** Correlation matrix of environmental variables of Tongoy Bay with *A. purpuratus* physiological rates. Significance values at a = 0.05 are shown by asterisks (*P*-value< 0.05). **(B)** Redundancy analysis (RDA) for environmental variables (i.e. Ekman transport, temperature, DO, and pH$_{NBS}$) with *A. purpuratus* physiological rates (i.e. GRs, NCRs, DCRs, and GCRs).

higher speed of loss of dissolved oxygen in the water column (i.e., upwelling rate) recorded in the *winter* and *spring* seasons may be explaining the higher variability in oxygen conditions. On average, seasonal pH values were also highly correlated with higher Ekman transport values. This agrees with previous studies that determine that multiple processes such as organic matter remineralization, high oxygen consumption, and dissolved inorganic carbon (DIC) production occur at deeper depths making upwelled waters poor in oxygen and rich pCO_2 concentrations (low pH) (Umasangaji et al., 2021). Average seasonal surface Chl-*a* at Tongoy Bay also responded to the radiation and temperature annual cycle (highest values recorded in *summer* and *spring* seasons). However, during the *winter* months, when stronger upwelling-favourable winds were recorded at PLV, a peak of Chl-*a* (with values ranging between 0.6 and 18.6 mg m^{-3}) was registered. This agrees with several studies across different upwelling systems showing how nearshore productivity is coupled to local upwelling conditions (e.g., Daneri et al., 2012; Du and Peterson, 2014; Aguirre et al., 2021).

Upwelling generates important coastal environmental fluctuations at local and larger scales as a consequence of deep upwelled waters properties (i.e., colder, hypoxic-anoxic, acidic) which, in many cases, can cause physiological constraints for marine biota. Paradoxically, these areas highlight by their high productivity, high biodiversity, and significant socio-economical contributions to humans (Carr et al., 2002; Chavez and Messié, 2009; Yáñez et al., 2017). In particular, the Humboldt Current System is recognized as one of the most productive areas on a global scale (300 gC/m^2 per year, Kämpf and Chapman, 2016) holding one of the highest fisheries worldwide (Chavez et al., 2008). Only in Chile in 2018, 3.7 million tons of fish (including mollusks and crustaceans) were captured with a value of USD 11,544.1 million being aquaculture responsible for 91% of this value (OECD, 2021). In particular, scallop aquaculture in Chile is an important socioeconomic activity whose production reached 7,600 tones in 2018 (SERNAPESCA, 2019) being exported to multiple international target markets (e.g. Spain, France, Singapore, and Brazil), and contributing to more than US$5.5 million to the Chilean's export basket (Yáñez et al., 2017). However, to date, the culture of *A. purpuratus* in Chile is completely carried out in the natural environment being highly vulnerable to environmental fluctuations and climate change impact-drivers.

Our study show how *A. purpuratus* physiology was significantly altered by seasonal environmental conditions which were modulated by the presence and intensity of favourable-upwelling winds. The lowest *A. purpuratus* performance (lowest GRs and GCRs) occurred during the *spring* season when upwelling generated an elevated number and intense cooling and de-oxygenation events resulting in rapid losses of temperature and oxygen in the water column. Environment imposes biological constraints (e.g., major energy requirement) which are especially notorious when habitat conditions reach values near (or out) of the physiological tolerance ranges of species (Pörtner, 2008). In particular, cold stress has

significant consequences from molecular to major physiological scales affecting cellular processes, development, metabolism, growth, and swimming capacities, among others (Pernet et al., 2007; Boroda et al., 2020). In addition, oxygen levels below physiological thresholds impact the performance, fitness, and behavior of the majority of marine taxa (e.g., Vaquer-Sunyer and Duarte, 2008). Previous studies on *A. purpuratus* show higher survivorship and growth under higher temperatures (Arntz et al., 2006) in agreement with Waller (1969) who described this species as warmed-adapted due to its tropical/sub-tropical origin. Also, more recent studies show how *A. purpuratus* is also seriously affected by hypoxia (e.g., lower growth and net calcification rates), especially when low oxygen conditions are also accompanied by changes in temperature or pH conditions (i.e., see Aguirre-Velarde et al., 2016; Ramajo et al., 2019; Ramajo et al., 2020). Indeed, multiple studies warn that low pH values are physiologically stressful for the majority of calcifying biota (Kroeker et al., 2013) affecting particularly calcification and metabolic rates, shell growth, and larval development among others (Kroeker et al., 2013). However, *A. purpuratus* living at Tongoy Bay seems to be highly adapted to acidified conditions (i.e., higher growth and calcification rates, see Ramajo et al., 2016) which have been attributed to acclimatization and local adaptation processes (Ramajo et al., 2016; Ramajo et al., 2019). Still, the magnitude and direction of changes in physiological responses to pH fluctuations depend greatly on temperature, oxygen, or food availability conditions (Ramajo et al., 2016; Lagos et al., 2016; Ramajo et al., 2019; Ramajo et al., 2020) which could explain the lowest GCRs observed during *spring* months when pH did not show the lowest values of the year, but oxygen and temperature showed important reductions.

Nevertheless, *A. purpuratus* was not only exposed to the most intense cooling and de-oxygenation events during the *spring* season but also to the most rapid reductions in temperature (cooling rate) and oxygen concentrations (de-oxygenation rate). Certainly, this had serious consequences on the physiological performance of this species (lowest GR and GCRs, and higher DRCs). Coping responses to physiological stress in marine organisms can take many shapes as they depend on the direction, duration, magnitude, and velocity of the environmental changes (Kristensen et al., 2020). In particular, the velocity of environmental changes is extremely relevant from the point of view of evolutionary processes and the expression of biological mechanisms, but also in the current context of climate change where unprecedented rapid changes are occurring in all world oceans (i.e., climate velocities, e.g., Brito-Morales et al., 2018).

Lower physiological performance during *spring* can be also explained by the annual environmental cycle as a continuous decrease in temperature, oxygen, and pH occurring from *summer* to *winter*, where *winter* also showed the lowest average temperatures, and oxygen and pH values. Continuous environmental changes and previous stressful conditions may have affected the total *A. purpuratus* energetic budget, and thus the ability to express physiological mechanisms to cope with

rapid changes in temperature and oxygen during *spring*. Fluctuating and stressful environmental conditions foster the expression of biological mechanisms that require high consumption of energy (Hendriks et al., 2015; Ramajo et al., 2020) which also promote the energetic requirements re-allocation and the apparition of physiological *trade-offs*, lower physiological performance, and decreased fitness (e.g., Pan et al., 2015). This may be explaining the steady decay in GRs, NCRs and GCRs observed during the experiment. On the other hand, food supply could also explain why *A. purpuratus* fitness was not affected during the *summer* and *spring* months, as both seasons also presented the highest food availability conditions (i.e., higher Chl-*a* concentrations). Previous studies have observed and suggested that *A. purpuratus* can increase its feeding rates under low pH (Ramajo et al., 2016) and after intense upwelling events to recover from physiological stressful conditions (see Ramajo et al., 2020).

Energetic demands for maintenance and reproduction change across sizes and ages (Kooijman, 2000). Thus, it can be expected that not all life-stages cope equally with environmental fluctuations as different life-stages present different necessities in terms of food, oxygen availability, and calcium carbonate supply (Baumann et al., 2012). Our study shows how seasonal physiological responses of *A. purpuratus* were significantly modulated by the size (age) (Table 1), especially when environmental conditions pose a physiologically stressful scenario with rapid cooling and deoxygenation/corrosive rates (i.e., *Spring* season, see Figure 7). S*ize* seems to be a key factor explaining the thermal tolerances of *A. purpuratus* which may explain different results among previous studies. Meanwhile, Arntz et al. (2006) and Lagos et al. (2016) studies detected a higher tolerance of *A. purpuratus* under higher than lower temperatures, Ramajo et al. (2019) concluded that *A. purpuratus* seems to be a species better adapted to cold than warmer conditions. These differences among studies may be attributed to differences in the life-stages tested as Arntz et al. (2006) and Lagos et al. (2016) studies were performed on larvae or adult organisms, while Ramajo et al. (2019) experiment was accomplished on juveniles. A similar physiological pattern has been observed to compare the physiological performance of juveniles and adults to changes in pH (see Ramajo et al., 2016; Lagos et al., 2016). Unfortunately, to date, no studies addressing the oxygen availability impact among different *A. purpuratus* life-stages have been yet performed.

The lower physiological performance observed in *A. purpuratus* adult stages as a consequence of more intense upwelling conditions occurring during the spring season may have additional impacts on aquaculture production as the scallop industry in Tongoy Bay mainly relies on natural larvae captured from the natural environment. Although *A. purpuratus* gametes release can occur throughout the year, this is more active in the austral spring and summer seasons when higher food availability (Chl-*a* concentrations) is present due to nutrients supplied by upwelling (Avendaño et al., 2008). However,

unusual intense upwelling events and related stressful conditions could have important impacts on the reproductive *A. purpuratus* conditions (i.e., gamete release, spawning time, as well as egg production and larval survivorship). Multiple studies in bivalve species show how temperature, pH, and oxygen conditions modulate multiple reproductive adult traits including larvae availability and their survivorship (i.e., Kroeker et al., 2013; Breitburg et al., 2018). In particular, for *A. purpuratus*, studies performed by Cantillánez et al. (2005, 2006, 2008) and Avendaño et al. (2005) show how dates of spawning events occur under higher water temperatures and food availability conditions. Here, although *A. purpuratus* reproductive-related traits were not addressed, our results (i.e., lower performance in older scallops) suggest that intense cooling and deoxygenation/corrosive conditions driven by intense upwelling events may constrain reproductive *A. purpuratus* cycle due to growth-maintenance-reproduction *trade-offs* which are more evident in older stages as energetic costs are size and volume-dependent (see the introduction for references).

In brief, our study concludes that physiological sensitivity to isolated environmental variables is not able to entirely explain the seasonal physiological performance of *A. purpuratus*. Upwelling imposes differential physiological pressures across *A. purpuratus* life-stages, where the combination of intensity and the velocity of the changes, as well as the food availability, modulated the performance and the energy available to cope with uninterrupted (and sometimes stressful) environmental conditions. This highlight the necessity of considering marine upwelling habitats as highly complex and heterogenous environmental entities where fluctuations ranges (and not only average values), the speed of changes, and the nature of the interaction (antagonist, synergistic, additive) among environmental variables need to be considered to make better projections about the future of fisheries and shell marine aquaculture (SMA) developed in EBUS (Henson et al., 2017; Kristensen et al., 2020). In particular, this is highly relevant along the Humboldt Current System, as the coastal invertebrates' catches have shown sustained growth since 1950, and specifically, SMA is a growing productive activity with an elevated socio-economic impact on the region and worldwide (FAO 2005-2021; Gutiérrez et al., 2017). However, to date, understanding how SMA in this region will cope with future climate conditions driven by changes in upwelling, ocean acidification, or ocean deoxygenation as a consequence of climate change is not completely understood as it requires an adequate comprehension of the environmental dynamics of marine systems, as well as, better knowledge about the physiological tolerance of the species and their different life-stages to heterogeneous conditions.

Data availability statement

The raw data supporting the conclusions of this article will be made available by the authors, without undue reservation.

Author contributions

Funding

Acknowledgments

Conflict of interest

Publisher's note

Supplementary material

The Supplementary Material for this article can be found online at: https://www.frontiersin.org/articles/10.3389/fmars.2022.992319/full#supplementary-material

References

Aguirre, C., García-Loyola, S., Testa, G., Silva, D., and Farias, L. (2018). Insight into anthropogenic forcing on coastal upwelling off south-central Chile. *Elem. Sci. Anth.* 6 (1), 59. doi: 10.1525/elementa.314

Aguirre-Velarde, A., Jean, F., Thouzeau, G., and Flye-Sainte-Marie, J. (2016). Effects of progressive hypoxia on oxygen uptake in juveniles of the Peruvian scallop, *Argopecten purpuratus* (Lamarck 1819). *Aquaculture* 451, 385–389. doi: 10.1016/j.aquaculture.2015.07.030

Aguirre, C., Garreaud, R., Belmar, L., Farías, L., Ramajo, L., and Barrera, F. (2021). High-Frequency Variability of the Surface Ocean Properties Off Central Chile During the Upwelling Season. *Front. Mar. Sci.* doi: 10.3389/fmars.2021.702051

Aravena, G., Broitman, B., and Stenseth, N. C. (2014). Twelve years of change in coastal upwelling along the central-northern coast of Chile: spatially heterogeneous responses to climatic variability. *PloS One* 9 (2), e90276. doi: 10.1371/journal.pone.0090276

Arntz, W. E., Gallardo, V. A., Gutiérrez, D., Isla, E., Levin, L. A., Mendo, J., et al (2006). El Niño and similar perturbation effects on the benthos of the Humboldt, California, and Benguela Current upwelling ecosystems. *Adv. Geosci.* 6, 243–265. doi: 10.5194/adgeo-6-243-2006

Avendaño, M., and Cantillánez, M. (2022). *Argopecten purpuratus* (Mollusca, pectinidae) post-El niño 1997-98 response in la rinconada marine reserve (Antofagasta, Chile). *Lat. Am. J. Aquat. Res.* 50 (2), 168–180. doi: 10.3856/vol50-issue2-fulltext-2776

Avendaño, M., Cantillánez, M., Le Pennec, M., and Thouzeau, G. (2008). Reproductive and larval cycle of the scallop argopecten purpuratus (Ostreoida: Pectinidae), during El niño-la niña events and normal weather conditions in antofagasta, Chile. *Rev. Biologia Trop.* 56 (1), 121–132.

Avendaño, M., Cantillánez, M., and Peña, J. (2006). Effect of immersion time of culthch on spatfall of the scallop argopecten purpuratus (Lamarck 1819) in the marine reserve at la rinconada, antofagasta, Chile. *Aquacul. Int.* 14, 267–283. doi: 10.1007/s10499-005-9033-y

Avendaño, M., Cantillánez, M., Rodríguez, L., Zúñiga, O., Escribano, R., and Oliva, M. (2005). *Crecimiento y estructura demográfica de Argopecten purpuratus en la reserva marina La Rinconada* (Antofagasta, Chile: Ciencias marina). 31 (3), 491–503.

Bakun, A., Black, B. A., Bograd, S. J., García-Reyes, M., Miller, A. J., Rykaczewski, R. R., et al (2015). Anticipated effects of climate change on coastal upwelling ecosystems. *Curr. Clim. Change Rep.* 1, 85–93. doi: 10.1007/s40641-015-0008-4

Bakun, A. (1975). *Daily and weekly upwelling indices, west coast of North Americ-73* (U.S: Department of Commerce), 114. Available at: https://repository.library.noaa.gov/view/noaa/15387.

Basilio, C. D., Cañete, J. I., and Rozbaczylo, N. (1995). Polydora sp. (Spionidae), un poliqueto perforador de las valvas del ostión argopecten purpuratus (Bivalvia: Pectinidae) en bahía tongoy, Chile. *Rev. Biologia Marina* 30, 71–77. doi: 10.4067/S0718-19572001000100009

Baumann, H., Talmage, S. C., and Gobler, J. (2012). Reduced early life growth and survival in a fish in direct response to increased carbon dioxide. *Nat. Clim. Change* 2, 38–41. doi: 10.1038/nclimate1291

Bayne, B. L., and Newell, R. C. (1983). Physiological Energetics of Marine Molluscs. Eds. Saleuddin, A. S. M, and Wilbur, K. M. B. T.-T. M. (Academic press), 407–515. doi: 10.1016/B978-0-12-751404-8.50017-7

Belmadani, A., Echevin, V., Codron, F., Takahashi, K., and Junquas, C. (2014). What dynamics drive future wind scenarios for coastal upwelling off Peru and Chile? *Clim. Dyn.* 43, 1893–1914. doi: 10.1007/s00382-013-2015-2

Bertrand, A., Lengaigne, M., Takahashi, K., Avadi, A., Poulain, F., and Harrod, C (2020). *El Niño southern oscillation (ENSO) effects on fisheries and aquaculture. FAO fisheries and aquaculture technical paper no. 660* (Rome: FAO). doi: 10.4060/ca8348en

Boroda, A. V., Kipryushina, Y. O., and Odintsova, N. A. (2020). The effects of cold stress on mytilus species in the natural environment. *Cell Stress Chaperones* 25 (6), 821–832. doi: 10.1007/s12192-020-01109-w

Bravo, L., Ramos, M., Astudillo, O., Dewitte, B., and Goubanova, K. (2016). Seasonal variability of the ekman transport and pumping in the upwelling system off central-northern Chile (∼ 30° s) based on a high-resolution atmospheric regional model (WRF). *Ocean Sci.* 12 (5), 1049–1065. doi: 10.5194/os-12-1049-2016

Breitburg, D., Levin, L. A., Oschlies, A., Grégoire, M., Chaves, F. P., Conley, D. J., et al (2018). Declining oxygen in the global ocean and coastal waters. *Science* 359 (6371), eaam7240. doi: 10.1126/science.aam7240

Brito-Morales, I., García-Molinos, J., Schoeman, D. S., Burrows, M. T., Poloczanska, E. S., Brown, C. J., et al (2018). Climate Velocity Can Inform Conservation in a Warming World. *Trends Ecol. Evol.* 33 (6), 441–457. doi: 10.1016/j.tree.2018.03.009

Byrne, M. (2012). Global change ecotoxicology: Identification of early life history bottlenecks in marine invertebrates, variable species responses and variable experimental approaches. *Mar. Environ. Res* 76, 3–15. doi: 10.1016/j.marenvres.2011.10.004

Cantillánez, M., Avendaño, M., Thouzeau, G., and Le Pennec, M. (2005). Reproductive cycle of argopecten purpuratus (Bivalvia: Pectinidae) in la rinconada marine reserve, (Antofagasta, chile): response to environmental effects of El niño and la niña. *Aquaculture* 246, 181–195. doi: 10.1016/j.aquaculture.2004.12.031

Carr, M.-E., Strub, P. T., Thomas, A. C., and Blanco, J. L. (2002). Evolutions of the 1996–1999 la niña and El niño conditions off the western coast of south America: a remote sensing perspective. *J. Geophys. Res.* 108 (C12), 3236. doi: 10.1029/2001JC001183

Chapman, P. (1996). Upwelling in the ocean: Modern processes and ancient records. *Limnology Oceanography* 41. doi: 10.4319/lo.1996.41.7.1585

Chauvaud, L., Patry, Y., Jolivet, A., Cam, E., Le Goff, C., Strand, Ø., et al (2012). Variation in size and growth of the great scallop pecten maximus along a latitudinal gradient. *PloS One* 7 (5), e37717. doi: 10.1371/journal.pone.0037717

Chavez, F. P., and Messié, M. (2009). A comparison of eastern boundary upwelling ecosystems. *Prog. Oceanogr.* 83, 80–96. doi: 10.1016/j.pocean.2009.07.032

Chavez, F. P., Bertrand, A., Guevara-Carrasco, R., Soler, P., and Csirke, J. (2008). The Northern Humboldt Current System: ocean dynamics, ecosystem processes, and fisheries. *Prog. Oceanogr* 79, 95–105. doi: 10.1016/j.pocean.2008.10.012

Clark, M. S., Peck, L. S., Arivalagan, J., Backeljau, T., Berland, S., Cardoso, J. C., et al (2020). Deciphering mollusc shell production: the roles of genetic mechanisms through to ecology, aquaculture and biomimetics. *Biol. Rev.* 95 (6), 1812–1837. doi: 10.1111/brv.12640

Clark, H. R., and Gobler, C. J. (2016). Diurnal fluctuations in CO2 and dissolved oxygen concentrations do not provide a refuge from hypoxia and acidification for early-life-stage bivalves. *Mar. Ecol. Prog. Ser.* 558, 1–14. doi: 10.3354/meps11852

Cury, P., and Roy, C. (1989). Optimal environmental window and pelagic fish recruitment success in upwelling areas. *Can. J. Fish. Aquat. Sci.* 46 (4), 670–680. doi: 10.1139/f89-086

Daneri, G., Lizárraga, L., Montero, P., González, H. E., and Tapia,. F. J. (2012). Wind forcing and short-term variability of phytoplankton and heterotrophic bacterioplankton in the coastal zone of the Concepción upwelling system (Central Chile). *Prog. Oceanography* 92–95, 92–96. doi: 10.1016/j.pocean.2011.07.013

Davies, P. S. (1989). Short-term growth measurements of corals using an accurate buoyant weighing technique. *Mar. Biol.* 101, 389–395. doi: 10.1007/BF00428135

Du, X., and Peterson, W. T. (2014). Seasonal Cycle of Phytoplankton Community Composition in the Coastal Upwelling System Off Central Oregon in 2009. *Estuaries Coasts* 37, 299–311. doi: 10.1007/s12237-013-9679-z

Falvey, M., and Garreaud, R. D. (2009). Regional cooling in a warming world: Recent temperature trends in the southeast pacific and along the west coast of subtropical south america, (1979–2006). *J. Geophys. Res.: Atmospheres* 114 (D4), D04102. doi: 10.1029/2008JD010519

FAO (2005-2021). "World inventory of fisheries. Subsidies and trade distortion. Issues Fact Sheets," in *Text by Audun Lem* (Rome: FAO Fisheries Division [online]).

Figueroa, D., and Moffat, C. (2000). On the influence of topography in the induction of coastal upwelling along the Chilean coast. *Geophys. Res. Lett.* 27 (23), 3905–3908. doi: 10.1029/1999GL011302

García-Reyes, M., Largier, J. L., and Sydeman, W. J. (2014). Synoptic-scale upwelling indices and predictions of phyto- and zooplankton populations. *Prog. Oceanogr.* 120, 177–188. doi: 10.1016/j.pocean.2013.08.004

García-Reyes, M., Sydeman, W. J., Schoeman, D. S., Rykaczewski, R. R., Black, B. A., Smit, A. J., et al (2015). Under Pressure: Climate Change, Upwelling, and Eastern Boundary Upwelling Ecosystems. *Front. Mar. Sci.* doi: 10.3389/fmars.2015.00109

Garreaud, R., and Muñoz, R. C. (2005). The low-level jet off the west coast of subtropical south America: Structure and variability. *Monthly Weather Rev.* 133 (8), 2246–2261. doi: 10.1175/MWR2972.1

Gaylord, B., Kroeker, K. J., Sunday, J. M., Anderson, K. M., Barry, J. P., Brown, N. E., et al (2015). Ocean acidification through the lens of ecological theory. *Ecology* 96 (1), 3–15. doi: 10.1890/14-0802.1

Gazeau, F., Parker, L. M., Comeau, S., Gattuso, J. P., O'Connor, W. A., Martin, S., et al (2013). Impacts of ocean acidification on marine shelled molluscs. *Mar. Biol.* 160, 2207–2245. doi: 10.1007/s00227-013-2219-3

Gutiérrez, D., Akester, M., and Naranjo, L. (2017). Productivity and Sustainable Management of the Humboldt Current Large Marine Ecosystem under climate change. *Environ. Dev.* 17, 126–144. doi: 10.1016/j.envdev.2015.11.004

Hendriks, I. E., Duarte, C. M., Olsen, Y. S., Steckbauer, A., Ramajo, L., Moore, T. S., et al (2015). Biological mechanisms supporting adaptation to ocean acidification in coastal ecosystems. *Estuarine Coast. Shelf Sci.* 152, A1–A8. doi: 10.1016/j.ecss.2014.07.019

Henson, S., Beaulieu, C., Ilyina, T., John, J. G., Long, M., Séférian, R., et al (2017). Rapid emergence of climate change in environmental drivers of marine ecosystems. *Nat. Commun.* 8, 14682. doi: 10.1038/ncomms14682

Huyer, A. (1983). Coastal upwelling in the California current system. *Prog. Oceanogr.* 12, 259–284. doi: 10.1016/0079-6611(83)90010-1

IPCC (2021). "Climate Change 2021: The Physical Science Basis. Contribution of Working Group I to the Sixth Assessment Report of the Intergovernmental Panel on Climate Change,". Eds. V. Masson-Delmotte, P. Zhai, A. Pirani, S. L. Connors, C. Péan, S. Berger, et al (Cambridge, United Kingdom and New York, NY, USA: Cambridge University Press). doi: 10.1017/9781009157896

Kämpf, J., and Chapman, P. (2016). *Upwelling systems of the world. A scientific journey to the most productive marine ecosystems* (Switzerland: Springer International Publishing). doi: 10.1007/978-3-319-42524-5

Kooijman, S (2000). *Dynamic Energy and Mass Budgets in Biological Systems* (2nd ed.). Cambridge: Cambridge University Press. doi: 10.1017/CBO9780511565403

Kristensen, T. N., Ketola, T., and Kronholm, I. (2020). Adaptation to environmental stress at different timescales. *Ann. N.Y. Acad. Sci.* 1476, 5–22. doi: 10.1111/nyas.13974

Kroeker, K. J., Kordas, R. L., Crim, R., Hendriks, I. E., Ramajo, L., Singh, G. S., et al (2013). Impacts of ocean acidification on marine organisms: quantifying sensitivities and interaction with warming. *Glob Change Biol* 19, 1884–1896. doi: 10.1111/gcb.12179

Lagos, N. A., Benítez, S., Duarte, C., Lardies, M. A., Broitman, B. R., Tapia, C., et al (2016). Effects of temperature and ocean acidification on shell characteristics of argopecten purpuratus: implications for scallop aquaculture in an upwelling-influenced area. *Aquacult. Environ. Interact.* 8, 357–370. doi: 10.3354/aei00183

Lagos, N. A., Benítez, S., Grenier, C., Rodriguez-Navarro, A. B., García-Herrera, C., Abarca-Ortega, A., et al (2021). Plasticity in organic composition maintains biomechanical performance in shells of juvenile scallops exposed to altered temperature and pH conditions. *Sci. Rep.* 11, 24201. doi: 10.1038/s41598-021-03532-0

Langer, G., Nehrke, G., Baggini, C., Rodolfo-Metalpa, R., Hall-Spencer, J. M., and Bijma, J. (2014). Limpets counteract ocean acidification induced shell corrosion by thickening of aragonitic shell layers. *Biogeosciences* 11, 7363–7368. doi: 10.5194/bg-11-7363-2014

Lardies, M. A., Benitez, S., Osores, S., Vargas, C. A., Duarte, C., Lohrmann, K. B., et al (2017). Physiological and histopathological impacts of increased carbon dioxide and temperature on the scallops argopecten purpuratus cultured under upwelling influences in northern Chile. *Aquaculture* 479, 455–466. doi: 10.1016/j.aquaculture.2017.06.008

Lluch-Cota, S. E., Hoegh-Guldberg, O., Karl, D., Pörtner, H. O., Sundby, S., and Gattuso, J. P. (2014). "Cross-chapter box on uncertain trends in major upwelling ecosystems," in *Climate change 2014: Impacts, adaptation, and vulnerability. part a: Global and sectoral aspects. contribution of working group II to the fifth assessment report of the intergovernmental panel of climate change*. Eds. C. B. Field, V. R. Barros, D. J. Dokken, K. J. Mach and M. D. Mastrandrea (Cambridge, Uk: New York, NY: Cambridge University Press), 149–151.

Lu, J., Vecchi, G. A., and Reichler, T. (2007). Expansion of the Hadley cell under global warming. *Geophys. Res. Lett.* 34, L06805. doi: 10.1029/2006GL028443

MacLeod, C. D., and Poulin, R. (2015). Interactive effects of parasitic infection and ocean acidification on the calcification of a marine gastropod. *Marine Ecology Progress Series*. 537, 137–150. doi: 10.1016/j.ijpara.2015.02.007

Moraga-Opazo, J., Valle-Levinson, A., Ramos, M., and Pizarro-Koch, M. (2011). Upwelling-triggered near-geostrophic recirculation in an equatorward facing embayment. *Continental Shelf Res.* 31 (19-20), 1991–1999. doi: 10.1016/j.csr.2011.10.002

OECD (2021). "The Organization for Economic Cooperation and Developmen)," in *Fisheries and Aquaculture in Chile January 2021* (Paris (France: . OECD Review of Fisheries Country Notes).

Palmer, A. R. (1981). Do carbonate skeletons limit the rate of body growth? *Nature* 292 (5819), 150–152. doi: 10.1038/292150a0

Pan, T. C. F., Applebaum, S. L., and Manahan, . D. T. (2015). Experimental ocean acidification alters the allocation of metabolic energy. *Proc. Natl. Acad. Sci.* 112 (15), 4696–4701. doi: 10.1073/pnas.1416967112

Pernet, F., Tremblay, R., Comeau, L., and Guderley, H. (2007). Temperature adaptation in two bivalve species from different thermal habitats: energetics and remodelling of membrane lipids. *J. Exp. Biol.* 210 (17), 2999–3014. doi: 10.1242/jeb.006007

Pörtner, H. (2008). Ecosystem effects of ocean acidification in times of ocean warming: a physiologist's view. *Mar. Ecol. Prog. Ser.* 373, 203–217. doi: 10.3354/meps07768

Rahn, D. A., and Garreaud, R. D. (2014). A synoptic climatology of the near-surface wind along the west coast of south America. *Int. J. Climatol.* 34 (3), 780–792. doi: 10.1002/joc.3724

Ramajo, L., Prado, L., Rodriguez-Navarro, A. B., Lardies, M. A., Duarte, C. M., and Lagos, N. A. (2016). Plasticity and trade-offs in physiological traits of intertidal mussels subjected to freshwater-induced environmental variation. *Mar. Ecol. Prog. Ser.* 553, 93–109. doi: 10.3354/meps11764

Ramajo, L., Fernández, C., Núñez, Y., Caballero, P., Lardies, M. A., and Poupin, M. J. (2019). Physiological responses of juvenile Chilean scallops (Argopecten purpuratus) to isolated and combined environmental drivers of coastal upwelling. *ICES J. Mar. Sci.* 76 (6), 1836–1849. doi: 10.1093/icesjms/fsz080

Ramajo, L., Valladares, M., Astudillo, O., Fernández, C., Rodríguez-Navarro, B. A., Watt-Arévalo, P., et al (2020). Upwelling intensity modulates the fitness and physiological performance of coastal species: Implications for the aquaculture of the scallop argopecten purpuratus in the Humboldt current system. *Sci. Total Environ* 745, 140949. doi: 10.1016/j.scitotenv.2020.140949

Renault, L., Dewitte, B., Falvey, M., Garreaud, R., Echevin, V., and Bonjean, F. (2009). Impact of atmospheric coastal jet off central Chile on sea surface temperature from satellite observations, (2000–2007). *J. Geophys. Res.* 114, C08006. doi: 10.1029/2008JC005083

Rutllant, J., and Montecino, V. (2002). Multiscale upwelling forcing cycles and biological response off north-central Chile. *Rev. Chil. Hist. Natural* 75 (217), e231. doi: 10.4067/S0716-078X2002000100020

Rykaczewski, R. R., Dunne, J. P., Sydeman, W. J., García-Reyes, M., Black, B. A., and Bograd, S. J. (2015). Poleward displacement of coastal upwelling-favorable winds in the ocean's eastern boundary currents through the 21st century. *Geophys. Res. Lett.* 42, 6424–6431. doi: 10.1002/2015GL064694

Schneider, W., Donoso, D., Garcés-Vargas, J., and Escribano, R. (2017). Water-column cooling and sea surface salinity increase in the upwelling region off central Chile driven by a pole-ward displacement of the south pacific high. *Prog. Oceanogr.* 151, 38–48. doi: 10.1016/j.pocean.2016.11.004

Seibel, B. A. (2011). Critical oxygen levels and metabolic suppression in oceanic oxygen minimum zones. *J. Exp. Biol.* 214 (2), 326–336. doi: 10.1242/jeb.049171

SERNAPESCA (2019) *Desembarque total*. Available at: http://www.sernapesca.cl/sites/default/files/2019_0301_desembarque_total.pdf (Accessed December 9, 2022).

Sprogis, K. R., Christiansen, F., Wandres, M., and Bejder, L. (2018). El Niño southern oscillation influences the abundance and movements of a marine top predator in coastal waters. *Glob Change Biol.* 24, 1085–1096. doi: 10.1111/gcb.13892

Strub, P. T., Shillington, F. A., James, C, and Weeks, S. J. (1998). Satellite comparison of the seasonal circulation in the Benguela and California current systems. *South African Journal of Marine Science*, 19 (1), 99-112. doi: 10.2989/025776198784126836

Sydeman, W. J., García-Reyes, M., Schoeman, D. S., Rykaczewski, R. R., Thompson, S. A., Black, B. A., et al (2014). Climate change and wind intensification in coastal upwelling ecosystems. *Science* 345 (6192), 77–80. doi: 10.1126/science.1251635

Talmage, S. C., and Gobler, ,. C. J. (2010). Effects of past, present, and future ocean carbon dioxide concentrations on the growth and survival of larval shellfish. *Proc. Natl. Acad. Sci.* 107 (40), 17246–17251. doi: 10.1073/pnas.0913804107

Tapia, F. J., Navarrete, S. A., Castillo, M., Menge, B. A., Castilla, J. C., Largier, J., et al (2009). Thermal indices of upwelling effects on inner-shelf habitats. *Prog. Oceanography* 83, 278–287. doi: 10.1016/j.pocean.2009.07.035

Thiel, M., et al (2007) *The Humboldt current system of northern and central Chile*. Available at: https://www.webofscience.com/wos/WOSCC/full-record/000252476600006.

Thompson, R. J., and MacDonald, B. A. (2006). "Chapter 8 Physiological integrations and energy partitioning," in S. E. Shumway and F. S. Parsons Eds. *Scallops: Biology, Ecology and Aquaculture.* (Elsevier), 35, 493–520. doi: 10.1016/S0167-9309(06)80035-9

Thomsen, J., Haynert, K., Wegner, K.M., and Melzner, F. (2015). Impact of seawater carbonate chemistry on the calcification of marine bivalves. *Biogeosciences* 12, 4209–4220. doi: 10.5194/bg-12-4209-2015

Torres, R., and Ampuero, P. (2009). Strong CO2 outgassing from high nutrient low chlorophyll coastal waters off central Chile (30 s): The role of dissolved iron. *Estuarine Coast. Shelf Sci.* 83 (2), 126–132. doi: 10.1016/j.ecss.2009.02.030

Torres, R., Turner, D. R., Silva, N., and Rutllant, J. (1999). High short-term variability of CO2 fluxes during an upwelling event off the Chilean coast at 30 s. *Deep Sea Res. Part I: Oceanogr. Res. Papers* 46 (7), 1161–1179. doi: 10.1016/S0967-0637(99)00003-5

Truebano, M., Fenner, P., Tills, O., Rundle, S. D., and Rezende, E. L. (2018). Thermal strategies vary with life history stage. *J. Exp. Biol.* 221 (8), jeb171629. doi: 10.1242/jeb.171629

Trussell, G. C., and Smith, L. D. (2000). Induced defenses in response to an invading crab predator: an explanation of historical and geographic phenotypic change. *Proc. Natl. Acad. Sci.* 97 (5), 2123–2127. doi: 10.1073/pnas.040423397

Umasangaji, H., and Ramili, Y. (2021). "Mini review: Characteristics of upwelling in several coastal areas in the world," in *IOP Conference Series: Earth and Environmental Science*, Vol. 890. 012004 (IOP Publishing). doi: 10.1088/1755-1315/890/1/012004

Vaquer-Sunyer, R., and Duarte, C. M. (2008). Thresholds of hypoxia for marine biodiversity. *Proc Natl Acad Sci U S A*. doi: 10.1073/pnas.0803833105

von Brand, E., Abarca, A., Merino, G. E., and Stotz, W. (2016). "Scallop fishery and aquaculture in Chile: A history of developments and declines," in *Scallop, biology, ecology, aquaculture and fisheries*. Eds. S. E. Shumway and J. G. (Oxford: Elsevier), 1047–1072. doi: 10.1016/B978-0-444-62710-0.00026-2

Waldbusser, G. G., Hales, B., Langdon, C. J., Haley, B., Schrader, P., Brunner, E. L., et al (2015). Ocean acidification has multiple modes of action on bivalve larvae. *PloS One* 10 (6), e0128376. doi: 10.1371/journal.pone.0128376

Waldbusser, G. G., Voigt, E. P., Bergschneider, H., Green, M. A., and Newell, R. I. E. (2011). Biocalcification in the Eastern oyster (Crassostrea virginica) in relation to long-term trends in Chesapeake bay pH. *Estuaries Coasts* 34, 221–231. doi: 10.1007/s12237-010-9307-0

Waller, T. R. (1969). The evolution of the *Argopecten gibbus* stock (Mollusca: Bivalvia), with emphasis on the Tertiary and Quaternary species of eastern North America. *Memoir (The Paleontological Society)* 3, i–125.

Wessel, N., Martin, S., Badou, A., Dubois, P., Huchette, S., Julia, V., et al (2018). Effect of CO2–induced ocean acidification on the early development and shell mineralization of the European abalone (Haliotis tuberculata). *J. Exp. Mar. Biol. Ecol* 508, 52–63. doi: 10.1016/j.jembe.2018.08.005

Yáñez, E., Lagos, N.A., Norambuena, R., Silva, C., Letelier, J., Muck, K.-P., et al (2017). Impacts of climate change on marine fisheries and aquaculture in Chile. *Climate Change Impacts Fish. Aquacult.: A Global Anal.* 1 (1), 239–342. doi: 10.1002/9781119154051.ch10

Zhao, X., Han, Y., Chen, B., Xia, B., Qu, K., and Liu, G. (2020). CO2-driven ocean acidification weakens mussel shell defense capacity and induces global molecular compensatory responses. *Chemosphere* 243, 125415. doi: 10.1016/j.chemosphere.2019.125415